



Research Article

Cyclic performance of emulative precast beam to column connection with corbel using dowel bar

Rajeswari M ¹, Jaya KP ²

¹ Department of Civil Engineering, PSG College of Technology, Coimbatore, Tamilnadu (India), rajiceg@gmail.com

² Division of Structural Engineering, Anna University Chennai - CEG campus, Chennai, Tamilnadu (India), kpjaya@nayan.co.in

*Correspondence: rajiceg@gmail.com

Received: 17.10.2021; **Accepted:** 05.08.2022; **Published:** 30.08.2022

Citation: Rajeswari, M. and Jaya K P. (2022). Cyclic performance of emulative precast beam to column connection with corbel using dowel bar. *Revista de la Construcción. Journal of Construction*, 21(2), 354-367. <https://doi.org/10.7764/RDLC.21.2.354>.

Abstract: The objective of this study is to examine the seismic performance of exterior and interior types of an emulative precast beam to column connection, constructed with grouted steel dowel bar and cast-in-situ concrete under quasi-static reversed cyclic loading. The dowel bar connection between the precast structural elements is achieved by inserting the dowel bar into the column corbel's holes and the precast portion of the beam. To secure the dowel bar's anchorage, these holes are packed with non-shrinkage grout and then cast-in-situ concreting is done in the joint core and the entire upper segment of the precast beam. In the past, particularly after an earthquake in the Emilia-Romagna region of Italy in May 2012 (Ercolino, Magliulo, & Manfredi, 2016), witnessed damage to precast reinforced concrete structures was more likely to occur in the precast beam-column joint section. Hence, it's essential to improve the performance of the beam-column joint to withstand all possible lateral load combinations, which are to be included in the design and detailing of the precast structural components. This study analyzed an eight-story RC frame building for earthquake loading using Staad.Pro software. The exterior and interior types of proposed beam-column connections were designed and detailed using the design forces and moments computed by the Staad.Pro analysis, in accordance with the Indian standard codes (IS 456, 2000), (IS 1893, 2016) and (IS 13920, 2016). The beam-column joint behavior under quasi-static cyclic loading was studied using one-third scaled-down test specimens, i.e., monolithic (MBC-EJ & MBC-IJ) and emulative beam-column (EBC-EJ & EBC-IJ) exterior and interior joints. In that proposed emulative connection, the structural continuity and compatibility between the precast elements were achieved through the corbel with the dowel bar and cast-in-situ concreting. The test specimen's ultimate and yield load carrying capacity, energy dissipation capacity, stiffness degradation, and ductility parameters were determined based on the obtained load-displacement hysteresis relationship. Based on the findings, the precast exterior joint specimens (EBC-EJ) were found to be 14.36% more ductile and 13.23% more energy dissipative than monolithic exterior joint specimens (MBC-EJ). Similarly, precast interior joint specimens (EBC-IJ) outperformed monolithic interior joint specimens (MBC-IJ) by 6.27% more ductility and 16.86% more energy dissipation. Therefore, the experimental results confirmed that using grouted dowel bars and wet concreting in the joint area enhances rigidity and structural continuity, as well as improves the ultimate strength of precast connections to a level that closely resembles typical monolithic beam-column joints.

Keywords: Precast beam-column, grout, dowel bar connection, cyclic loading, seismic behavior.

1. Introduction

When incorporating precast elements into a structural system (ACI 550.2R-13, 2013), the deformations and stresses that occur in and around the connections must be taken into account to prevent structural damage during seismic loading. Precast concrete members should be joined effectively to ensure the connection's strength (more than or equal to the member strength), adequate inelastic deformation capability, and energy dissipation capacity. The joints in the precast structural system (Elliott, 2016) were classified into two types: dry or mechanical joints and wet or emulative joints. In dry or mechanical connections, precast structural elements are joined with each other using anchors, fasteners, bolts, or welding, reinforcing steel bar, grout, and steel sections such as angles, plates, etc. In wet or cast-in-situ connections, the connections are mainly formed by using cast-in-situ concreting and rebar splicing. Among these types, wet connections will provide excellent performance against lateral loads as they tend to behave monolithically and provide continuity and structural integrity in the precast structural system.

Generally, pinned dowel bar connections are designed as hinged joints, which is applicable only for low-rise buildings subjected to gravity (static) loading. During an earthquake, the major role of pinned dowel bar connections is to retain the beam seating over the precast column while transferring lateral loads between the precast structural elements (Ercolino, Magliulo & Manfredi, 2016). But in the case of high relative rotation between the columns and beams, the shear strength and moment transfer of connections are limited. As a result, they are not suitable for use in highly earthquake-prone areas (Blandón & Rodríguez, 2005). Instead, if these pinned connections are modified into rigid or semi-rigid connections (Kremmyda, Fahjan, & Tsoukantas, 2014), they can be used for high seismicity areas by ensuring enough structural continuity and moment transfer between the elements. Hence, the proposed emulative beam-column connection belongs to the wet type, which is developed by using a dowel bar connection between corbel and beam, and in-situ concreting is applied in the joint core and the upper portion of the precast beam to maintain the structural integrity between the precast elements.

2. Literature review

The various research studies that have been conducted in the thrust area of the dowel bar connection between beam and column over the last decade (2010–2021) are summarized below in chronological order. Aguiar et al. (2012) examined the potential factors that influence the seismic performance of grouted dowels used in connecting the precast structural elements. They took into account the four test variables, such as the diameter of the dowel bars (16, 20, and 25 mm), the inclination of the dowel bar (0° , 45° , and 60°) orthogonal to the joint interface, the existence of axial compressive loads right-angled to the interface, and the concrete crushing strength adjoining the dowel bar. From the experimental outcomes (Aguiar, Bellucio, & El Debs, 2012), the inclined dowel bar has significantly higher shear resistance compared to the perpendicular dowel bar; and the contribution of the dowel bar to the plastic hinge formation is about 98% (0° inclination), on average 45% (45° inclination), and on average 35% (60° inclination) of the total dowel capacity. Fischinger et al. (2012) investigated the beam-column dowel connections undergoing significant relative rotations using parameters such as the number of dowels, the amount of confinement around the dowel bars, and their distance from the edges of columns and beams. Due to large relative rotations (Fischinger, Zoubek, Kramar, & Isaković, 2012), the dowel in the joint interface undergoes failure before the column.

Zoubek et al. (2013) analyzed the cyclic behavior of dowel connections, which are extensively used in low-rise industrial precast structures. During cyclic loading, the plastic hinge formed at a shallower depth, and the high relative rotation that occurred in the beam and column reduced the connection strength by 15 to 25% (Zoubek, Isakovic, Fahjan & Fischinger, 2013). In these types of connections, the use of a neoprene bearing pad at the interface has increased the connection strength. Vidjeapriya et al. (2013) studied the cyclic response of precast mechanical beam-column connections utilizing dowel bars with cleat angles under cyclic loading. In that, the RC monolithic beam-column junction was outperformed by the dowel bar with a cleat angle connection due to its superior performance in the areas of energy dissipation and ductility (Vidjeapriya, Vasanthalakshmi & Jaya, 2013).

Magliulo et al. (2014) performed a non-linear finite element analysis on various analytical models of monolithic reinforced concrete B-C dowel connections under monotonic shear loading to understand the influence of different dowel bar sizes and

adjacent concrete cover thickness (frontal and lateral side of dowel bar). The results confirmed that the greater frontal concrete cover reduces the tensile stress in the concrete, which prevents side-splitting, and an increase in the lateral concrete cover leads to a better confining effect (Magliulo, Ercolino, Cimmino, Capozzi & Manfredi, 2014). Parastesh et al. (2014) developed a ductile moment-resistant interior and exterior beam-column connection suitable for a highly seismically active area. The spacing and type of stirrup (open and closed type) in the connection zone were considered as the test variables. In comparison to monolithic connections, the proposed specimens exhibited degradation of strength and stiffness at drift ratios greater than 3% in the open stirrup and up to 4% in the closed stirrup, as well as higher energy dissipation capacity (30%) and ductility (up to 46%). As a result (Parastesh, Hajirasouliha, & Ramezani, 2014), the provision of a cross-inclined bar in the joint region delays the onset of diagonal fracture in the cyclically loaded joint. According to a study by Nimse et al. (2014) the wet precast beam-column subassembly using RC corbels with dowel bars has significantly larger ductility and 33.3% higher load carrying capacity than a monolithic beam-column subassembly under progressive collapse loading conditions (Nimse, Joshi, & Patel, 2014).

Yuksel et al. (2015) assessed the seismic behavior of external precast beam-column connections employed in industrial and residential building applications. Based on the ductility ratios obtained in the experimental study (Ercan Yuksel, Faruk Karadogan H, Engin Bal I, Alper Ilki, Ahmet Bal, & Pinar Inci, 2015), the connections were classified as low ductility (industrial) and medium ductility (residential) connections. These connections exhibited a stable hysteretic loop at 2% drift, and at around 3% drift, the strength degradation and significant pinching in the joint were observed. Kremmyda et al. (2017) proposed an analytical expression to predict the horizontal shear resisting capacity of precast RC pinned dowel connections that takes into account the effects of various parameters such as pre-compressive stress in the dowel bar, loading condition (monotonic or cyclic loads), number of dowel bars and their diameter, material strength (concrete, steel, grout), and strength of cover concrete near the dowel bar. The proposed expression addresses the two cases, i.e., the dowel bar yielding associated with concrete crushing ($D > 6d_b$) belongs to failure mode I (Local Failure) and splitting of concrete occurs in the direction of load or side-splitting perpendicular to the load direction ($D < 6d_b$) confirms failure mode II (Global Failure). However, in the case of $D < 6d_b$, the confining stirrup contribution around the dowel bar can change the failure mode to ductile from brittle (Kremmyda, Fahjan, Psycharis, & Tsoukantas, 2017).

Isakovic et al. (2019) evaluated the global failure mechanism in dowel bar connections through the strut and tie model approach (Isakovic, Zoubek, & Fischinger, 2019). Zhou et al. (2019) investigated the behavior of half-scaled, fully assembled precast concrete subassemblies using corbels and dowel bar connection (dry connection) for progressive collapse loading. The failure of the RC subassembly was due to the formation of plastic hinges in the longitudinal bars of the beam, whereas the failure of the precast specimens was due to dowel bar rupture and joint failure, which reduced the ultimate load resistance and displacement capacity to, on average, 78% and 75% of the RC specimens, respectively. In the middle column removal scenario during the progressive collapse (Yun Zhou, Taiping Chen, Yilin Pei, Hyeong-Jong Hwang, Xiang Hu, Weijian Yi, & Lu Deng, 2019), the load-carrying capacity in precast specimens was drastically reduced due to the rupture of dowel bars. This study shows that the CTA (Catenary Tension Action) and CCA (Compressive Arch Action) performance of precast specimens is better when high-strength, large-diameter dowel bars are used. Ahmed Tarabia et al. (2019) investigated the behavior of two-third scaled models of bolted connection type precast RC beam-column specimens under cyclic loading. They considered two variables in this study to enhance the shear resistance capability of exterior bolted connections through the provision of a shear key and shear reinforcement at the connection zone. Furthermore, the connection length measured from the face of the column and the location of the threaded bars were also taken into account. Based on the experimental findings (A. Tarabia, Allam, Etman, & Aboelhassan, 2019), precast specimens with shear reinforcement added toward the shear key vicinity had higher bending resistance, drift capacity, initial stiffness, ductility, and energy dissipation capacity than other precast and monolithic specimens.

Ghayeb et al. (2020) provided an in-depth review of dowel bar connections deployed in precast concrete buildings, as well as highlighted past research findings of various authors, including the failure mechanism in the dowel connections (Ghayeb, Razak, & Ramli Sulong, 2020). To predict the cyclic behavior of bolted-type precast reinforced beam-column connections. Ahmed Tarabia et al. (2021) proposed a non-linear finite element model that takes into account the effects of reinforcing bar slip, relative rotation, in-elastic shear response, and interface shear transfer in the beam-column joint. According to the verified

model results, the precast bolted connection with shear reinforcement in the shear key zone had about 50% less shear slip, more initial stiffness, and better energy dissipation than the precast bolted specimen without shear reinforcement (A. M. Tarabia, Etman, Allam, & Aboelhasan, 2021).

Based on a review of the existing literature, a lot of studies have been carried out on the pinned dowel connection with various parameters such as diameter, number, and eccentricity of dowel bars, effect of confinement reinforcement, frontal and lateral cover thickness, etc., but merely limited information exists on the performance of rigid dowel bar connections. According to Eurocode 8, the pinned beam-column dowel connections are designed using the capacity rule, which states that connections must remain in the elastic stage while developing the ultimate plastic moment of resistance in the column's critical region. As a result, pinned beam-column connections are designed as "over-designed connections" and are limited to low-rise structures due to their lower seismic resistance (EN 1992-1-1, 2004). Hence, the scope of this research is to comprehend the behavior of rigid dowel bar connections between the precast beams and column with corbel in a multi-storied frame located in a moderate seismicity area.

3. Experimental program

In this study, a G+7-storey RC Frame building was analyzed for all the possible loadings using Staad.Pro software. The building was considered to be located in Chennai, which falls under the Zone 3 category. The zone factor and the response reduction factor for this modelled building were 0.16 (Chennai) and 5. The modelled building was classified under "general buildings," so the importance factor for the building was 1. The type of soil present in this region was moderately stiff (medium type soil); hence the damping ratio was taken as 0.05. The typical and bottom story heights of the building were 4.11 m and 3.2 m, respectively. The design incorporates the yield strength of the reinforcing bar as 500 N/mm² and the concrete characteristic strength as 30 N/mm². The sectional properties of the beam, interior, and exterior columns were 300 mm x 450 mm, 300 mm x 600 mm, and 300 mm x 450 mm. The various loads, such as dead load, imposed load, and earthquake loads were considered for the analysis of the building and the load combinations were considered as per the Indian standard specifications (IS 456, 2000), (IS 1893, 2016). The critical load combination (1.5DL+1.5EQY) of the column and the design forces and moments in the critical connection region were determined from the Staad.Pro analysis is used to design and detail the monolithic (MBC-EJ and MBC-IJ) and emulative (EBC-EJ and EBC-IJ) exterior and interior beam-column joints. The three-dimensional and elevation views showing the exterior critical column of the modelled building are shown in Figure 1.

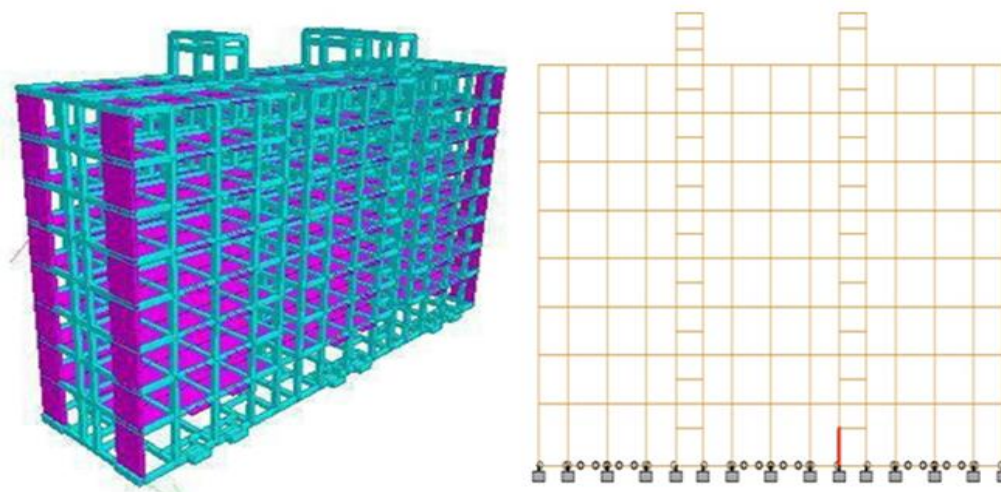


Figure 1. Three-dimensional view of modelled building and elevation view showing the exterior critical column of the modelled building.

3.1. Design and detailing of monolithic and precast specimens

In interior joint specimens (MBC-IJ and EBC-IJ), the beams are designed for an ultimate shear force (V_u) of 121.4 kN and an ultimate moment (M_u) of 160.9 kNm, whereas the columns are designed for an axial load (P_u) of 1975.4 kN and an ultimate moment (M_u) of 160.9 kNm. Furthermore, the exterior joint specimens (MBC-EJ and EBC-EJ) are designed to withstand the ultimate axial, shear, and moment loads of 1975.4 kN (P_u), 138.7 kN (V_u) and 184.4 kNm (M_u) obtained from the Staad.Pro analysis of an eight-storey RC-Framed building. The detailing of reinforcement is done as per IS 456:2000 and IS 13920:2016, respectively. The longitudinal reinforcement of 2#-20mm ϕ at the top, 4#-20mm ϕ at the bottom and the 8mm diameter lateral ties at a spacing of 150 mm c/c is provided (ϕ and # denote the diameter and number of bars) except where the beam requires the special confining reinforcement. The special confining reinforcement of 8mm diameter lateral ties (IS 13920:2016, cl.7.4.1) is provided over a length l_0 of 600 mm from each joint face, 75 mm center-to-center (c/c) towards mid span is provided in the beam. The longitudinal reinforcement of six numbers of 20 mm diameter bars is distributed evenly on all four sides, and the transverse reinforcement of 12 mm diameter bars at 150 mm c/c is provided in the column. The special confining reinforcement of 8 mm diameter lateral ties is given at a spacing of 75 mm c/c at a distance of 600 mm from the joint face. The development length of 1080mm is provided for the beam bar anchorage in to the column. The shear span a_v and the bearing width of the corbel are 100 mm and 300 mm, which are designed for an ultimate vertical load (maximum reaction from the beam) and a horizontal load of 120 kN and 18 kN. The main reinforcement of 3#-16mm ϕ and a shear link of 3#-10mm ϕ at 100mm c/c is provided in the corbel. The yield stress, diameter and development length of the dowel rod used in the emulative connection are 500 N/mm², 20 mm and 300 mm. The horizontal force is carried by the dowel in double shear and bending is ignored as the dowel is fully grouted in. The strength of the grout used in the design is 60 N/mm². The shear capacity of the dowel bar obtained based on equation (5) is 94.2 kN, which is greater than the design maximum shear force (70 kN). Hence, the dowel bar is safe against shear. Table 1 shows the theoretical ultimate resistance of dowel connections subjected to cyclic loading in which equations (1 to 4) are suitable for the pinned dowel bar connections, and equation (5) is suitable for rigid dowel bar connections.

Table 1. Theoretical ultimate resistance of dowel connections under cyclic loading.

Literature/Manual	Proposed expressions	Equation No.	Shear capacity of dowel bar
(E. N. Vintzeleou and T. P. Tassios, 1987)	$R_u = 0.65 \phi^2 \sqrt{f_{ck} f_y}$	(1)	31.84 kN
CNR 10025/98 (E. N. Vintzeleou and T. P. Tassios, 1987)	$V_{Rd} = 1.2 d_b^2 \sqrt{f_{yd} f_{cd}}$	(2)	44.76 kN
SAFECAST Project by NTUA (Bournas, Negro, & Molina, 2013)	For small rotations between elements $R_{u,sr} = 1.1 d_b^2 \sqrt{f_y \cdot f_{cc}}$	(3)	53.88 kN
	For large rotations between elements $R_{u,tr} = 0.9 d_b^2 \sqrt{f_y \cdot f_{cc}}$	(4)	44.09 kN
(Elliott, 2016)	$V_d = 0.6 f_y A_s \cos \alpha$ (α – the inclination of dowel bar)	(5)	94.20 kN

3.2. Scaling of prototype specimen

The model or test specimen is achieved by scaling down the prototype with a ratio of 1:3. The length scale factor is 3, the area and force scale factor is 9, and the moment scale factor is 27. The reinforcement detailing of the scaled-down models of the exterior and interior connections of the monolithic and emulative beam-column joints is shown in Figure 2.

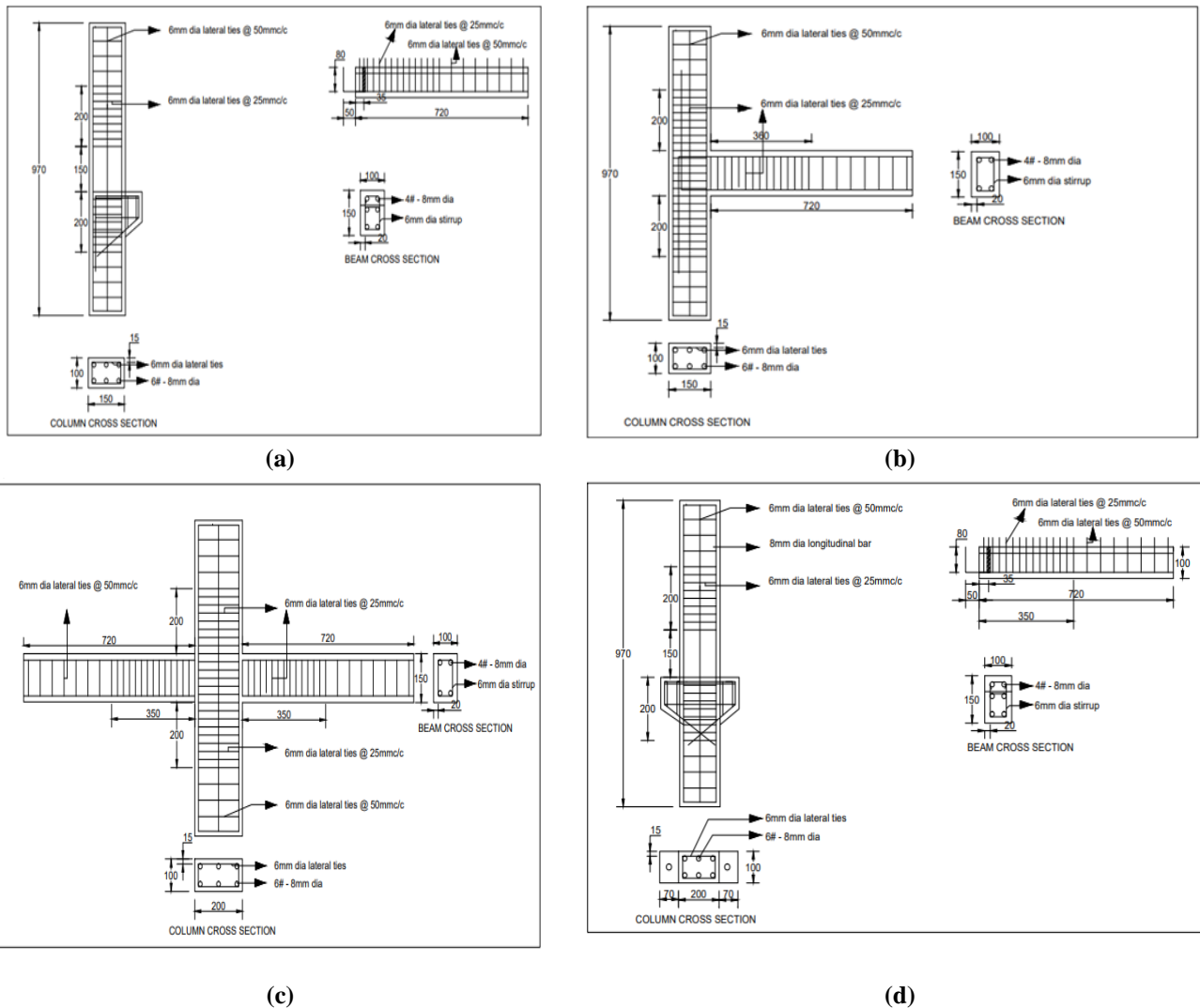


Figure 2. Reinforcement detailing of model specimens A) MBC-EJ specimen B) EBC-EJ specimen C) MBC-IJ specimen D) EBC-IJ specimen.

3.3. Casting of specimens

An emulative precast beam-column exterior connection (EBC-EJ) is comprised of corbels, grouted dowel bar, 90° bent up beam longitudinal bar, and cast-in-situ topping over the precast beam and the joint. At the site, the exterior connection (EBC-EJ) was formed by positioning the precast beam over the corbel using the dowel bar connection. Finally, the sleeve hole in the precast beam was grouted and cast-in-situ concreting was applied in the joint region and the top portion of the precast beam. Similarly, an emulative precast beam-column interior connection (EBC-IJ) consists of corbels, grouted dowel bars, continuity bars running throughout the beam, and on-site concreting over the precast beam and the joint. After erecting the precast beam over the corbel using the dowel bar, the sleeve hole in the precast beam was grouted. After placing the beam continuity bar at the site, cast-in-situ pouring was applied throughout the top portion of the precast beam and the joint region. The monolithic and precast emulative specimens cast at the site are shown in Figures 3(a) and 3(b).

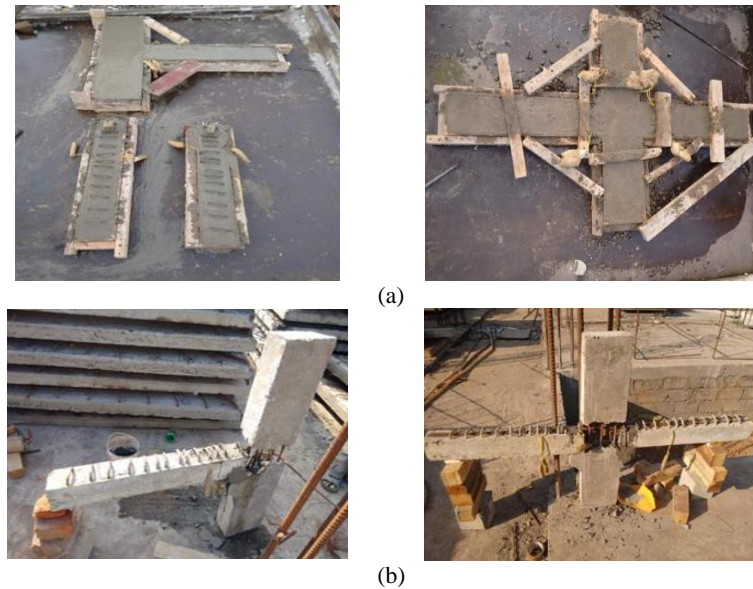


Figure 3. Casting of interior and exterior joint specimens, (a) Monolithic beam-column connection (MBC-EJ and MBC-IJ), (b) Emulative precast beam-column connection (EBC-EJ and EBC-IJ).

3.4. Experimental test up and instrumentation

A 2000 kN capacity loading frame was used for testing the beam-column joint specimens. The test specimens were loaded by a hydraulic actuator (1000 kN) on the column top to stimulate the building's gravity. Then the reverse cyclic loading was applied with the help of two hydraulic jacks and a load cell. The column was placed above the hinge support to stimulate the real boundary conditions. The capacities of the hydraulic jack under push (positive direction of loading) and pull (negative direction of loading) were 500 kN and 200 kN, respectively. The cyclic loading history applied to the exterior and interior specimens is shown in Figure 4. In exterior joints, the hydraulic jack was mounted on the beam's upper portion, and in the case of interior joints, the hydraulic jack was mounted on both the right and left sides of the beam, as shown in Figures 5(a) and 5(b). Dial gauges were fitted to the ends of the beam and the applied displacement was measured. The displacement-controlled seismic load in the interior joints was simulated by applying a push load on the right and a pull load on the left side of the beam, or vice versa, in the subsequent cycles, and in exterior joints, the consecutive push and pull were applied at the ends of the beam.

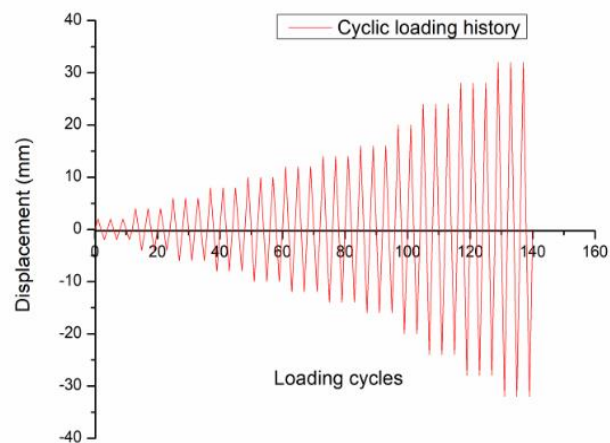


Figure 4. Cyclic loading history applied in the specimens.

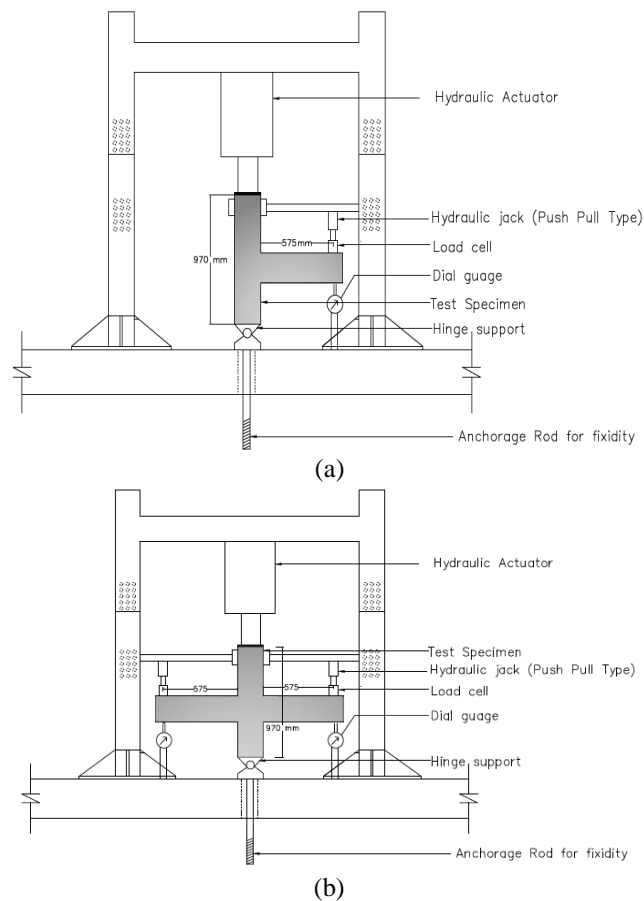


Figure 5. Experimental test setup for beam-column joint specimen, (a) exterior joint (b) Interior joint.

4. Experimental results and analysis

4.1 Load displacement hysteretic relationship

4.1.1. Exterior connection

Figure 6 shows the average load versus displacement hysteretic relationship curve of monolithic and precast emulative beam-column joint specimens (MBC-EJ, EBC-EJ, MBC-IJ, and EBC-IJ). In the monolithic beam-column exterior connection (MBC-EJ), the experimental ultimate load (13.2 kN) was attained in both the +20 mm and -20 mm displacement cycles. Beyond the 20 mm displacement cycle, there was strength degradation in both the positive and negative cycle directions. Consequently, the cracks started propagating and the crack width increased in the subsequent load cycles. Meanwhile, the shear cracks were prevented by the special confining reinforcement applied across the length of l_0 (200 mm) of each joint face. As a result, the flexural tensile cracks primarily occurred over the adjoining joint face region to an extent of 150 mm from the joint face. For this reason, the shear cracks were formed at the core of the exterior joint and the flexural tension cracks largely occurred over the adjacent joint face region.

In an emulative precast beam-column connection (EBC-EJ), the experimental ultimate load (12.5 kN) was attained in the +28 mm displacement cycle. Strength degradation commenced in the positive cycle direction at a 28mm displacement cycle, but in the negative cycle direction, it occurred beyond a 24mm displacement cycle. Due to further subsequent load cycles

after the strength degradation, the diagonal cracks started propagating from the bottom of the corbel near the dowel bar towards the joint region indicating the complete failure of the dowel bar connection, as depicted in Figure 7a. The dowel bar transfers the lateral load through the shear action between the precast elements and induces the non-uniform stress distribution in the concrete. In this straight dowel bar connection, the plastic hinge was formed at both the corbel and the precast portion of the beam.

4.1.2. Interior connection

In the monolithic beam-column interior connection (MBC-IJ), the experimental ultimate load (15 kN) was attained in the +24 mm displacement cycle. Furthermore, the degradation of strength occurred in both loading directions after the 24 mm displacement cycle. To prevent shear cracks in the vicinity of the joint face area, special confining reinforcement was provided throughout the length of l_0 (200mm) of each joint face. In the emulative beam-column interior connection (EBC-IJ), the experimental ultimate load (13.6 kN) was attained in the +28 mm displacement cycle. It is observed that the strength degradation occurs only after a 28 mm displacement cycle in both loading directions due to the presence of the corbel and dowel bar connection. Further subsequent load cycles result in extensive cracking at the interface of the joint due to the large relative rotation that occurs between the precast beam and the precast column element, which is depicted in Figure 7b.

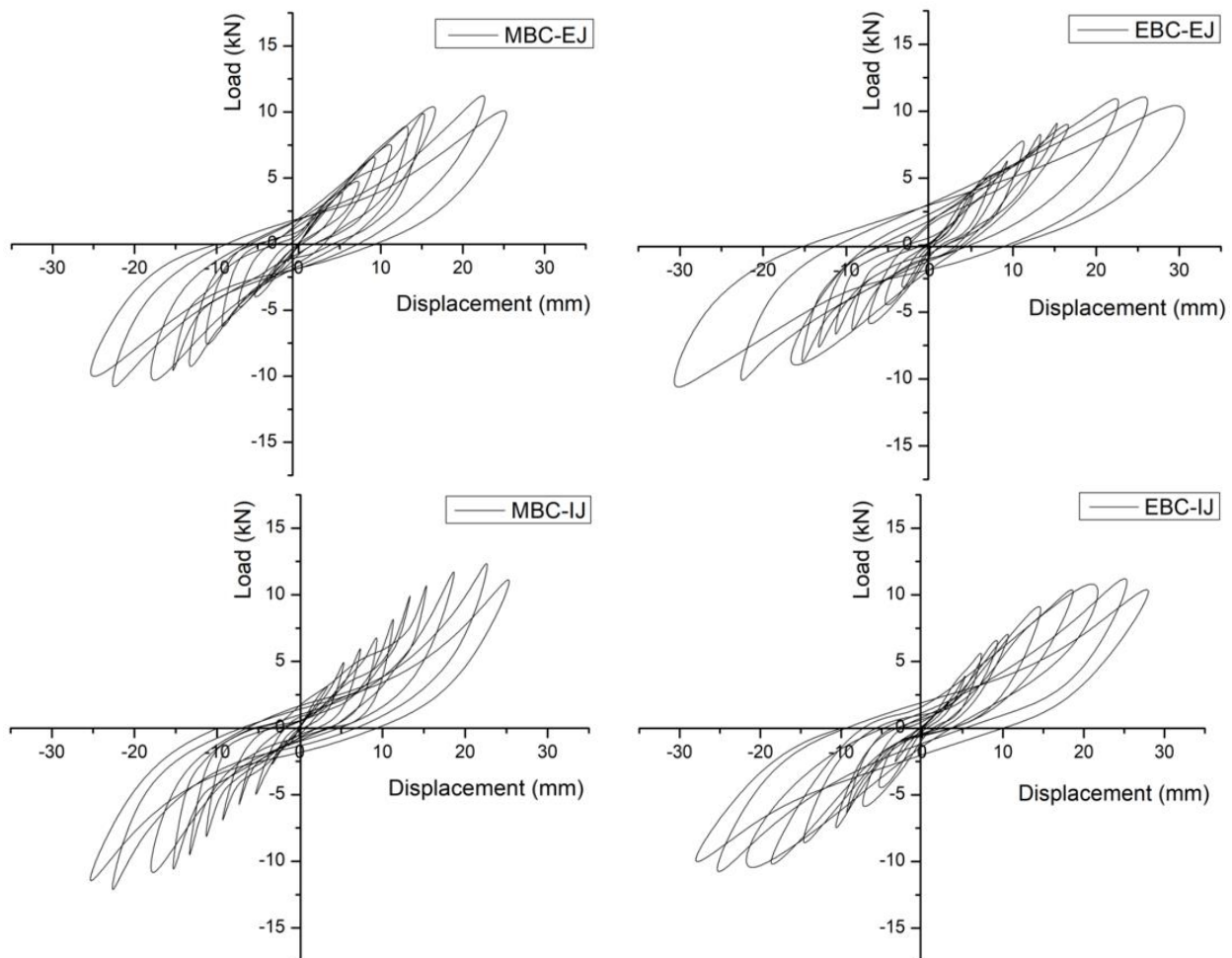


Figure 6. Hysteresis curve of exterior (MBC-EJ, EBC-EJ) and interior joint specimens (MBC-IJ, EBC-IJ).

4.2 The load-carrying capacity of specimens

Figure 8 presents the load versus displacement envelope curves of monolithic and emulative joint specimens. Table 2 shows the average peak load, average yield load and comparison of predicted and experimentally obtained ultimate flexural capacities of the monolithic and emulative beam-column joint specimens based on the load-displacement envelope curve. The yield point and ultimate point in a load versus displacement curve were obtained using the procedure followed in the ASTM code E2126-11. The R_u is the ratio between the experimental and theoretically calculated ultimate flexural capacities of the beam. The average ultimate and yield strength of the MBC-EJ specimen were 7.78% and 7.76% greater than the EBC-EJ specimen, respectively whereas the MBC-IJ specimen was 11.23% and 11.19 % greater than the EBC-IJ specimen in the interior joint. Therefore, the monolithic specimens performed significantly better in terms of load resistance than the emulative specimens. The strength degradation in the emulative precast connection was mainly due to the large rotation between the beams and columns.



Figure 7. (a) Damages observed in the MBC-EJ and EBC-EJ Specimen, (b) relative rotation between the beams and column of MBC-IJ specimen observed during experimentation.

Table 2. Test results of the monolithic and precast specimens.

Specimen details	Average yield load P_y (kN)	Average peak load P_{peak} (kN)	Yield moment M_y (kNm)	Peak moment M_{peak} (kNm)	$R_u = \frac{M_{peak,experimental}}{M_{peak,calculated}}$
MBC-EJ	5.28	13.20	3.04	7.59	1.11
EBC- EJ	4.90	12.25	2.82	7.04	1.03
MBC- IJ	5.96	14.90	3.43	8.57	1.44
EBC- IJ	5.36	13.40	3.08	7.71	1.29

4.3 Ductility

The displacement ductility factors of monolithic and emulative specimens are compared in Table 3. The emulative exterior and interior joint specimens exhibited 14.36% and 6.69% more ductility compared to the monolithic exterior and interior joint specimens. Due to higher ductility compared to monolithic specimens, the precast interior and exterior joint specimens can withstand more damage due to larger post-yielding deformation.

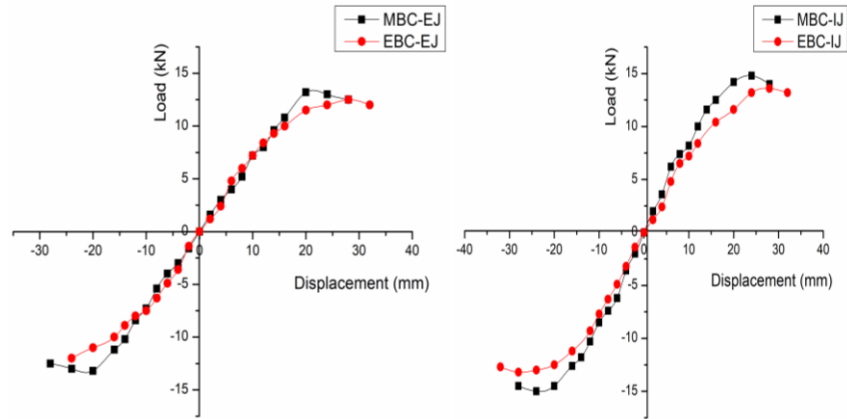


Figure 8 Comparison of envelope curves of exterior and interior joint specimens.

Table 3. Ductility factor of tested specimens.

Specimen	Yield displacement Δ_y (mm)		Ultimate displacement Δ_u (mm)		Displacement ductility factor		Average ductility factor
	Push	Pull	Push	Pull	Push	Pull	
MBC-EJ	6.00	7.40	16.6	16	2.76	2.16	2.46
EBC-EJ	6.23	5.8	17.5	16.4	2.81	2.83	2.82
MBC-IJ	5.75	5.77	16.28	16.45	2.83	2.85	2.84
EBC-IJ	6.58	6.57	19.86	20	3.01	3.04	3.03

4.4 Energy dissipation capacity

The "area under the load-displacement curves" is defined as the potential dissipated energy of a joint. Figure 9(a) and 9(b) show the comparison of energy dissipated in each displacement cycle of exterior joints (MBC-EJ and EBC-EJ) and interior joint specimens (EBC-EJ and EBC-IJ). Figure 9 (c) presents the cumulative energy dissipation capacity of monolithic and emulative specimens. Due to the predefined gap between the precast structural elements, it was found that the precast specimens dissipate more energy than the monolithic specimens beyond the 20 mm displacement cycle. The precast exterior and interior joint specimens have 13.23% and 16.06% more energy dissipation capacity than monolithic exterior and interior joint specimens, respectively. Hence, the precast specimen exhibited good energy dissipation compared to the monolithic specimen.

4.5 Stiffness degradation

Multiple cyclic load reversals cause the beam-column joint's stiffness to degrade, resulting in cracks and bond deterioration. The degree of stiffness degradation is dependent on material properties, joint dimension, and the amount of ductile detailing in the joint, the type of connection, and the loading history. Due to increases in crack growth, the rigidity decreased continuously as displacement levels increased. The secant stiffness is defined as "the slope of the line connecting the peak positive response to the peak negative response of the displacement-controlled load cycle". Normalized stiffness values were calculated for each specimen by comparing its initial stiffness measured at a displacement level of 2 mm. Figure 10 compares the normalized stiffness degradation of all specimens. The normalized stiffness degradation for the MBC-EJ, EBC-EJ, MBC-IJ, and EBC-IJ specimens obtained at the 28mm displacement level was 54.6%, 57.2%, 49.1%, and 52%, respectively. Compared to monolithic exterior (MBC-EJ) and interior joint specimens (MBC-IJ), the precast exterior (EBC-EJ) and interior joint (EBC-IJ) specimens exhibited a little higher loss of initial stiffness due to the more post-yielding deformation capability of the joint.

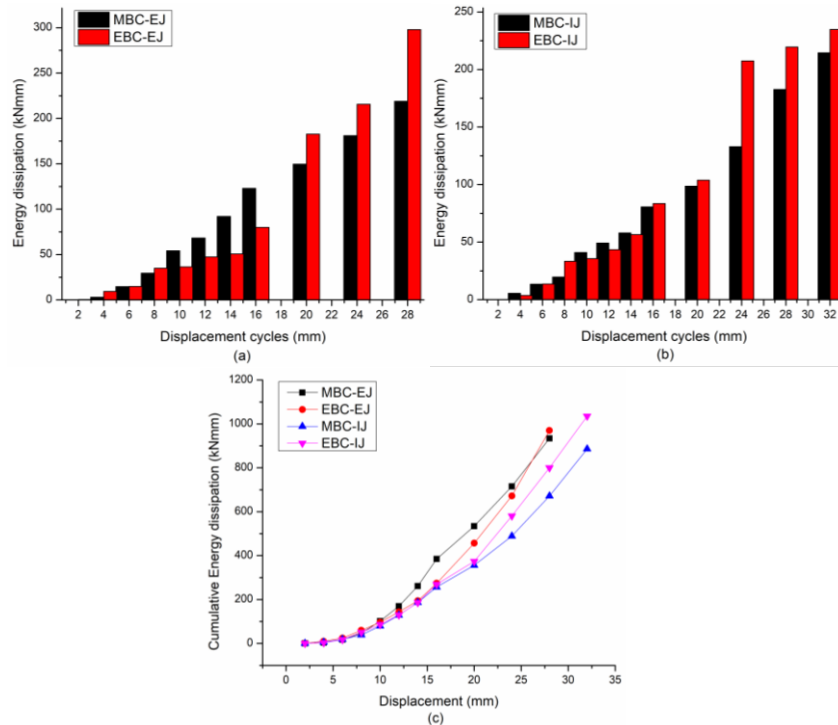


Figure 9. Comparison of the energy dissipation involved in each displacement cycle (a) Exterior joint specimens (MBC-EJ and EBC-EJ) (b) Interior joint specimens (EBC-EJ and EBC-IJ) (c) Cumulative energy dissipation of all specimens

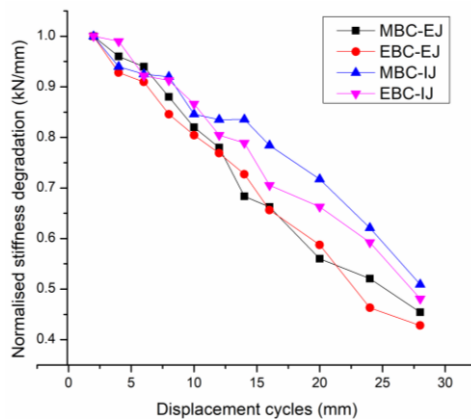


Figure 10. Comparison of Normalized stiffness degradation of all specimens.

5. Conclusions and comments

The important parameters that control the seismic resistance of moment-resistant building frames, such as ultimate and yield load carrying capacity, energy dissipation capacity, stiffness degradation, and ductility were considered to examine the seismic behaviour of exterior and interior beam-column joints of monolithic (MBC-EJ and MBC-IJ) and emulative precast specimens (EBC-EJ and EBC-IJ). Based on the observations made from the experimental investigation, the following conclusions were developed.

Grouted concrete plays a vital role in protecting the dowel reinforcement bar from the vulnerable damage resulting from lateral cyclic loading. In addition, the high-strength grout of M60 grade used in the cast hole sleeve controls the slippage of the dowel bar through bonding action and intensely controls the early failure of the dowel bar connection.

The ultimate strength of the MBC-IJ specimen was 11.23% greater than the EBC-IJ specimen, and the MBC-EJ specimen was 7.78 % greater than the EBC-EJ specimen. These results evidenced that the use of grouted steel reinforcing bar and wet concreting in the joint area of the emulative precast connection provides greater rigidity and structural continuity, thereby enhancing the ultimate load strength of precast connections i.e., nearly emulating the performance similar to conventional monolithic beam-column joints.

The precast specimen dissipates more energy than the monolithic specimen. In the case of the precast exterior (EBC-EJ) and interior joints (EBC-IJ), it was 13.23 % and 16.86 % higher than the monolithic specimen (MBC-EJ and MBC-IJ), respectively. As a result, the induced seismic excitations can be dissipated very effectively via the emulative joint.

The precast emulative exterior (EBC-EJ) and interior beam-column joint specimens were found to be more ductile than monolithic specimens (MBC-EJ and MBC-IJ) by 14.36% and 6.27%, respectively. Due to higher ductility compared to monolithic specimens, the precast interior and exterior joint specimens can withstand more damage due to larger post-yielding deformation. Therefore, the emulative connections have been preferred in RC structural frames subjected to moderate seismic events.

Therefore, it is concluded that cast-in-place connections using corbel with dowel bar performed better than monolithic specimens with respect to ductility and energy dissipation capacity.

Author contributions: Conceptualization and methodology: MR and KPJ; experimental investigation and drafting: MR; review, supervision, and enhancement of manuscript: MR and KPJ.

Funding: Authors self-funded the research.

Acknowledgments: This research work was carried out at the Structural dynamics laboratory, Division of structural engineering, Anna University, Chennai. The authors acknowledged the support rendered by Anna University, Chennai.

Conflicts of interest: The authors of this research declare that they have no conflicting interests in its publication.

References

- ACI 550.2R-13. (2013). Design guide for Connections in Precast Jointed Systems. Joint ACI-ASCE Committee 550, American Concrete Institute
- ASTM E2126-11. (2012). Standard Test Methods for Cyclic (Reversed) Load Test for Shear Resistance of Vertical elements of the Lateral Force Resisting Systems for Buildings
- Aguiar, E. A. B., Bellucio, E. K., & Debs, M. K. El. (2012). Behavior of grouted dowels used in precast concrete connections. *Structural Concrete*, 13(2), 84–94. <https://doi.org/10.1002/suco.201100048>
- Blandón, J. J., & Rodríguez, M. E. (2005). Behavior of Connections and Floor Diaphragms in Seismic-Resisting Precast Concrete Buildings. *PCI Journal*, 50(2), 56–75. <https://doi.org/10.15554/pcij.03012005.56.75>
- Bourmas, D. A., Negro, P., & Molina, F. J. (2013). Pseudodynamic tests on a full-scale 3-storey precast concrete building: Behavior of the mechanical connections and floor diaphragms. *Engineering Structures*, 57, 609–627. <https://doi.org/10.1016/j.engstruct.2013.05.046>
- Elliott, K. S. (2016). *Precast Concrete Structures* (Second edition). CRC Press.
- EN 1992-1-1. (2004). Design of concrete structures - Part 1-1. General rules and rules for buildings.
- Ercolino, M., Magliulo, G., & Manfredi, G. (2016). Failure of a precast RC building due to Emilia-Romagna earthquakes. *Engineering Structures*, 118, 262–273. <https://doi.org/10.1016/j.engstruct.2016.03.054>
- Fischinger, M., Zoubek, B., Kramar, M., & Isaković, T. (2012). Cyclic response of dowel connections in precast structures. 15th World Conference on Earthquake Engineering.

- Ghayeb, H. H., Razak, H. A., & Ramli Sulong, N. H. (2020). Performance of dowel beam-to-column connections for precast concrete systems under seismic loads: A review. *Construction and Building Materials*, 237, 1-25. <https://doi.org/10.1016/j.conbuildmat.2019.117582>
- IS 13920. (2016). Code of Practice for Ductile Detailing of Reinforced Concrete Structures Subjected to Seismic Forces. Bureau of Indian Standards, New Delhi, India.
- IS 1893. (2016). Code of practice for criteria for earthquake resistant design of structures-General Provisions and Buildings. Bureau of Indian Standards, New Delhi, India.
- IS 456. (2000). Indian Standard Code of Practice for Plain and Reinforced Concrete. Bureau of Indian Standards, New Delhi, India.
- Isakovic, T., Zoubek, B., & Fischinger, M. (2019). Cyclic capacity of dowel connections. In *Geotechnical, Geological and Earthquake Engineering (Vol. 47)*. https://doi.org/10.1007/978-3-319-78187-7_11
- Kremmyda, G. D., Fahjan, Y. M., Psycharis, I. N., & Tsoukantas, S. G. (2017). Numerical investigation of the resistance of precast RC pinned beam-to-column connections under shear loading. *Earthquake Engineering and Structural Dynamics*, 46(9), 1511–1529. <https://doi.org/10.1002/eqe.2868>
- Kremmyda, G. D., Fahjan, Y. M., & Tsoukantas, S. G. (2014). Nonlinear FE analysis of precast RC pinned beam-to-column connections under monotonic and cyclic shear loading. *Bulletin of Earthquake Engineering*, 12(4), 1615–1638. <https://doi.org/10.1007/s10518-013-9560-2>
- Magliulo, G., Ercolino, M., Cimmino, M., Capozzi, V., & Manfredi, G. (2014). FEM analysis of the strength of RC beam-to-column dowel connections under monotonic actions. *Construction and Building Materials*, 69, 271–284. <https://doi.org/10.1016/j.conbuildmat.2014.07.036>
- Nimse, R. B., Joshi, D. D., & Patel, P. V. (2014). Behavior of wet precast beam column connections under progressive collapse scenario: an experimental study. *International Journal of Advanced Structural Engineering*, 6(4), 149–159. <https://doi.org/10.1007/s40091-014-0072-3>
- Parastesh, H., Hajirasouliha, I., & Ramezani, R. (2014). A new ductile moment-resisting connection for precast concrete frames in seismic regions: An experimental investigation. *Engineering Structures*, 70, 144–157. <https://doi.org/10.1016/j.engstruct.2014.04.001>
- Tarabia, A., Allam, S., Etman, E., & Aboelhassan, M. (2019). Behavior of precast reinforced concrete beam-column external connections under cyclic loading. *WIT Transactions on the Built Environment*, 185, PII-27-PII-43. <https://doi.org/10.2495/ERES190031>
- Tarabia, A. M., Etman, E. E., Allam, S. M., & Aboelhassan, M. G. (2021). Modeling of Precast Reinforced Concrete Beam-column Joints Under Cyclic Loading. *Journal of Earthquake Engineering*, 1–30. <https://doi.org/10.1080/13632469.2021.1964651>
- Vidjeapriya, R., Vasanthalakshmi, V., & Jaya, K. P. (2013). Performance of exterior precast concrete beam-column dowel connections under cyclic loading. *International Journal of Civil Engineering*, 12(1 A), 82–94.
- Vintzeleou, E. N., & Tassios, T. P. (1987). Behavior of Dowels Under Cyclic Deformations. *Structural Journal*, 84(1), 18–30.
- Yuksel, E., Karadogan, H. F., Bal, I. E., Ilki, A., Bal, A., & Inci, P. (2015). Seismic behavior of two exterior beam-column connections made of normal-strength concrete developed for precast construction. *Engineering Structures*, 99, 157–172. <https://doi.org/10.1016/j.engstruct.2015.04.044>
- Zhou, Y., Chen, T., Pei, Y., Hwang, H. J., Hu, X., Yi, W., & Deng, L. (2019). Static load test on progressive collapse resistance of fully assembled precast concrete frame structure. *Engineering Structures*, 200, 1-14. <https://doi.org/10.1016/j.engstruct.2019.109719>
- Zoubek, B., Isakovic, T., Fahjan, Y., & Fischinger, M. (2013). Cyclic failure analysis of the beam-to-column dowel connections in precast industrial buildings. *Engineering Structures*, 52, 179–191. <https://doi.org/10.1016/j.engstruct.2013.02.028>



Copyright (c) 2022 Rajeswari, M. and Jaya K P. This work is licensed under a [Creative Commons Attribution-Noncommercial-No Derivatives 4.0 International License](https://creativecommons.org/licenses/by-nc-nd/4.0/).